ARTICLES

Tunneling dynamics of squeezed states in a potential well

A. Lenef and S. C. Rand
Division of Applied Physics, 1049 Randall Laboratory, University of Michigan, Ann Arbor, Michigan 48109-1120
(Received 6 August 1993)

WKB calculations have revealed that tunneling dynamics of localized wave packets in simple potential wells depend sensitively on the degree of squeezing of the wave function. Squeezed states are shown to tunnel more slowly in general than eigenstates of the well and states which are initially localized near the bottom of a well have much lower tunneling rates than states localized at the sides of the well. The dependence of tunneling time on energy also exhibits steps related to quasi-bound-state energies in a complex way. Additionally, modulations in the tunneling probability correlate with the motion of the squeezed wave packet in the well. These results have implications both for the dynamics of squeezed radiation fields and squeezed matter states, and examples of applications to controlled vibrational-state chemistry, ultralow-noise measurements of weak signals with Josephson junctions, and optical crystals are discussed.

PACS number(s): 03.65.Ge, 32.80.Pj, 42.50.Dv

I. INTRODUCTION

Theoretical work on the class of minimum-uncertainty states known as squeezed states was initiated as early as the 1920s [1], and revived in the context of quantum optics in the 1960s [2]. However, it as not until 1995 that experimental methods were developed to generate, propagate, and detect squeezed states of the radiation field [3]. This caused an immense increase of interest in the field. To date, schemes used to generate squeezed light have included four-wave mixing in atomic vapor, four-wave mixing in fibers, second-order parametric interactions in nonlinear crystals, and pump-noise-suppressed lasers [4–6]. It has been shown that squeezed states are important for sub-shot-noise-limited interferometry and spectroscopy with sensitivity below the shot-noise limit, and quantum nondemolition measurements. As a consequence of these applications and improved understanding of the uncertainty limits of quantum measurement, interest has grown recently in the possibility of creating squeezed states of matter which may similarly exhibit unusual and useful properties [7].

In this work, the effect of squeezing on tunneling from a simple potential well to a continuum of final states is investigated. The treatment is sufficiently general to apply to squeezed states of both radiation and matter fields. However, it is primarily motivated by an interest in modifications of tunneling phenomena due to localization of matter wave packets within potential wells. Several previous studies have analyzed tunneling of squeezed states in double well quantum oscillators [8,9], but have not been extended to describe transport. Here we analyze the evolution of squeezed states in a one-dimensional parabolic well with an infinite barrier on one side and a finite barrier on the other, explicitly incorporating the concept of transport. We show that squeezing of spatial coordinates can have a significant effect on tunneling probability and introduces structure in the dependence of tunneling time on energy of the wave packet which is related to the occurrence of quasibound states. Some of the implications of the sensitivity of tunneling probability to squeezing in the context of controlled vibrational-state chemistry, macroscopic quantum tunneling, and in optical crystals are discussed.

Calculations presented in the next section use a WKB procedure to obtain wave functions and the tunneling propagator for a parabolic well coupled to a continuum region of constant potential energy. Analytic expressions are obtained for wave functions and tunneling probabilities when the system is initially prepared in a squeezed state. Subsequently we examine the case of a cubic barrier, explain the relationship between localization, quasibound states, and tunneling probability, and discuss several applications.

II. TUNNELING BY A SQUEEZED STATE

A. Wave functions

The tunneling region considered in this paper is depicted in Fig. 1, where five distinct regions (I–V) are identified for convenience. A particle with average energy E is assumed to be initially localized in the potential well on the left and tunnels into the classically allowed region on the right which is terminated by a boundary at $x=L$. The maximum potential of the barrier is denoted by V_0. The points a, b, and c are the classical turning points. In the classically allowed region beyond the barrier, the potential falls to zero at $x=w$, and maintains a constant value $-\phi$ for $x>d$, where ϕ is assumed to be positive. The potential energy in the well region (region II of Fig. 1) is assumed to be harmonic:

$$V_{\parallel}(x)=\tfrac{1}{2}m\omega_0^2x^2 \ . \tag{1}$$

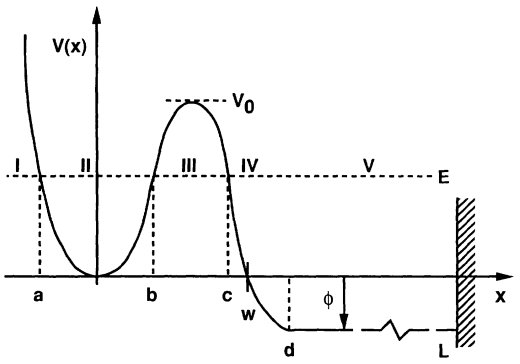

FIG. 1. Schematic of the potential well considered in this work, coupled to continuum of states at constant potential $-\phi$ and bounded by an infinite potential at $x=L$. Turning points for energy E are at $x=a$, b, and c.

Here, m is the particle mass, ω_0 is the frequency of oscillation, and x is the particle position. A characteristic length α^{-1} can be defined for the linear harmonic oscillator (LHO) wave functions corresponding to this potential well. This localization length gives the standard deviation of the particle position in the LHO ground state and is a useful quantity for discussing normalization and density of states:

$$\alpha=\sqrt{2m\omega_0/\hbar}\ . \tag{2}$$

The time evolution of a wave packet Ψ initially localized in the well is given by

$$\Psi(x,t)=\int_{-\infty}^{\infty} G(x',x;t)\Psi(x',0)dx'\ , \tag{3}$$

where $G(x',x;t)$ is the propagator which accounts for the evolution of the wave function from its initial value $\Psi(x',0)$ at time zero and position x' to its later value $\Psi(x,t)$ at time t and position x. The propagator $G(x',x;t)$ is given by

$$G(x',x;t)=\sum_k \psi_k^*(x')\psi_k(x)e^{-iE_k t/\hbar}\ . \tag{4}$$

Here, the sum is over wave vectors k in the continuum region, $x>d$, which are defined by

$$k=\sqrt{(2m/\hbar^2)(E_k+\phi)}\ . \tag{5}$$

The energies E_k of the eigenstates $\psi_k(x)$ for the potential $V(x)$ in Fig. 1 are a discrete set derived from the boundary conditions $\psi_k(L)=\psi_k(-\infty)=0$.

To obtain a simple analytic form for the propagator, we consider only states with energies which lie below the barrier peak V_0 and use a WKB approach. We neglect those states with energies close to V_0 for which the WKB approximation with linear turning points is not valid. For example, the WKB approximation breaks down for states within about $\hbar\omega_0$ of the barrier peak in a cubic potential containing roughly ten quasibound states. For moderate amounts of squeezing and energies limited to those below V_0, this condition restricts the average energy of the wave packet to within two or three $\hbar\omega_0$ below the top of the barrier.

Upon applying the appropriate connection formulas for linear turning points [10], the WKB eigenstates $\psi_k(x)$ with energies $0<E_k<V_0$ are of the form

$$\psi_k(x)=A_0U_k(x)\ , \tag{6}$$

where A_0 is a normalization constant. The unnormalized WKB solutions for the potential shown in Fig. 1 are given by

$$U_k^{\rm I}(x)=\frac{1}{\sqrt{Q}}\exp\left[-\int_x^a Q\,dx'\right],\quad x<a \tag{7}$$

$$U_k^{\rm II}(x)=\frac{2}{\sqrt{q}}\cos\left[\int_a^x q\,dx'-\frac{\pi}{4}\right],\quad a<x<b \tag{8}$$

$$U_k^{\rm III}(x)=\frac{1}{\sqrt{Q}}\sin\xi\exp\left[-\int_b^x Q\,dx'\right]+\frac{2}{\sqrt{Q}}\cos\xi\exp\left[\int_b^x Q\,dx'\right],\quad b<x<c \tag{9}$$

$$U_k^{\rm IV}(x)=\frac{\theta^{-1}}{\sqrt{q}}\sin\xi\cos\left[\int_c^x q\,dx'+\frac{\pi}{4}\right]+\frac{4\theta}{\sqrt{q}}\cos\xi\cos\left[\int_c^x q\,dx'-\frac{\pi}{4}\right],\quad c<x<d\ . \tag{10}$$

In the continuum region we find

$$U_k^{\rm V}(x)=\frac{2}{\sqrt{k}}\left[4\theta^2\cos^2\xi+\frac{1}{4}\theta^{-2}\sin^2\xi\right]^{1/2}\times\cos\left[k(x-d)+\eta+\varphi-\frac{\pi}{4}\right],\quad x>d \tag{11}$$

where the phase factor φ is given by

$$\varphi=\tan^{-1}\left[\frac{\theta^{-2}}{4}\tan\xi\right]\ . \tag{12}$$

The wave vectors for the classically allowed and forbidden regions near the origin are

$$q(x)=\alpha\sqrt{[E_k-V(x)]/\hbar\omega_0},\quad x<d \tag{13}$$

and

$$Q(x)=\alpha\sqrt{[V(x)-E_k]/\hbar\omega_0},\quad x<d \tag{14}$$

respectively. In these expressions, we have made convenient use of a barrier parameter θ defined by

$$\theta=\exp\left[\int_b^c Q\,dx'\right]\ . \tag{15}$$

The inverse of θ^2 is the tunneling probability for an eigenstate with energy E_k. Phases accumulated between turning points in the classically allowed region have been designated by

$$\xi=\int_a^b q\,dx' \tag{16}$$

and

$$\eta=\int_c^d q\,dx'\ . \tag{17}$$

For a parabolic well, ξ has the particularly simple form

$$\xi=\frac{\pi E_k}{\hbar\omega_0}\equiv\frac{\pi\omega_k}{\omega_0} . \tag{18}$$

An examination of Eq. (11) reveals that the probability of the particle being found in the continuum region is close to zero for particular values of the phase parameter ξ, namely $\xi=(n+\frac{1}{2})\pi$, where n is an integer. Particles with these phases are strongly localized in the well in quasibound states which, according to Eq. (18), occur almost exactly at the LHO eigenenergies and are easily seen to have narrow energy widths on the order of $\hbar\omega_0\theta^{-2}$. For energies below the bottom of the well ($-\phi<E_k<0$), the WKB wave functions decay exponentially for $x<c$ and can be neglected in the propagator [Eq. (4)] for the case of wave packets initially localized in the well.

The normalization constant A_0 is easily determined from Eqs. (6) and (11) for wave-packet energies far from LHO eigenenergies when L is large. However, near quasi-bound-state resonances, the probability amplitude in the well region is very sensitive to energy if the condition

$$L\gg\alpha^{-1}\theta^2 \tag{19}$$

cannot be satisfied. For modest values of $\theta\approx10^4$, Eq. (19) implies that L must be on the order of centimeters if the localization of the wave packet within a well a few angstroms in size is to be meaningful. As a consequence, we consider off-resonant and near-resonant cases separately (Appendix A), finding

$$A_0=\begin{cases}\left[\dfrac{k}{2L}\right]^{1/2}\left[4\theta^2\cos^2\xi+\dfrac{1}{4}\theta^{-2}\sin^2\xi\right]^{-1/2}, & \xi\neq\pi(n+\frac{1}{2})\\ \left[4\pi\alpha^{-2}+\dfrac{2L}{k}\left[4\theta^2\cos^2\xi+\dfrac{1}{4}\theta^{-2}\sin^2\xi\right]\right]^{-1/2}, & \xi\approx\pi(n+\frac{1}{2}) .\end{cases} \tag{20}$$

B. Density of states and the propagator

The determination of the density of states for evaluating the propagator requires similar considerations. Applying the boundary condition $\psi_k(L)=0$ to Eq. (11) implies $k(L-d)+\eta+\varphi-\pi/4=(n+\frac{1}{2})\pi$. The density of states is then given by the derivative of this quantization condition:

$$\frac{dn}{dk}=\frac{1}{\pi}\left[(L-d)+\frac{d\eta}{dk}+\frac{d\varphi}{dk}\right] . \tag{21}$$

Far from resonance, only the first term is significant in the limit of large L. However, as seen from Eq. (12), the phase φ also displays strong resonant behavior near the LHO eigenenergies. Including both of these terms for the general case gives the density of states

$$\frac{dn}{dk}=\frac{L}{\pi}+\frac{2k\alpha^{-2}}{4\theta^2\cos^2\xi+\frac{1}{4}\theta^{-2}\sin^2\xi} . \tag{22}$$

The propagator can now be evaluated by replacing the summation over k in Eq. (4) by an integral over the density of states. Applying the results of Eqs. (6), (20), and (22) yields the following expression for the propagator, valid both for on-resonance and off-resonance conditions:

$$G(x',x;t)=\frac{1}{2\pi}\int\frac{ke^{-iE_kt/\hbar}U_k^*(x')U_k(x)}{4\theta^2\cos^2\xi+\frac{1}{4}\theta^{-2}\sin^2\xi}dk, \quad x>d . \tag{23}$$

The denominator in the integrand of Eq. (23) becomes strongly resonant at quasi-bound-state energies. Only states $\psi_k(x)$ near these energies make important contributions to the integral. Moreover, since the initial wave functions are assumed to be strongly localized in the well, these states can be replaced by the LHO Hermite-Gaussian wave functions with appropriate normalization (Appendix A). With a change of variable from k to ω, the propagator becomes

$$G(x',x;t)=\frac{\alpha}{2\pi^{1/2}\omega_0}\sum_{n=0}^{N}(-1)^n\psi_n^{\mathrm{LHO}}(x')\int_{n\omega_0}^{(n+1)\omega_0}k^{-1/2}e^{-i\omega t}\left\{\frac{e^{i[k(x-d)+\eta-i\pi/4]}}{2\theta\cos\xi-(i/2)\theta^{-1}\sin\xi}+\text{c.c.}\right\}d\omega ,$$
$$x'<c, \quad x>d . \tag{24}$$

Here, the remaining summation is over the N quasibound states that lie below the barrier for which the WKB and parabolic approximations are valid.

The denominators in the integrand of Eq. (24) can be expanded about each resonance and are well approximated by simple poles. For $\xi\approx(n+\frac{1}{2})\pi$, the denominators can be written as

$$\frac{1}{2\theta\cos\xi\pm(i/2)\theta^{-1}\sin\xi}\cong(-1)^{n+1}\frac{\Gamma_n\theta_n}{[\omega-(n+\frac{1}{2})\omega_0]\pm i(\Gamma_n/2)} , \tag{25}$$

where

$$\Gamma_n = \frac{\omega_0}{2\pi\theta_n^2} \ . \tag{26}$$

In this approximation, we ignore frequency shifts on the order of $\omega_0\theta^{-4}$ and higher-order imaginary contributions which introduce corrections to these first-order quasibound-state decay rates. Note that we have also made explicit use of the parabolic well assumption.

To complete the evaluation of Eq. (24), we expand the phase η about frequency $\omega=(n+\frac{1}{2})\omega_0$. From Eq. (17), we find

$$\eta=\eta_n+\tau_n[\omega-(n+\tfrac{1}{2})\omega_0] \ , \tag{27}$$

where

$$\eta_n=\alpha\int_c^d\sqrt{(n+\tfrac{1}{2})-V(x')/\hbar\omega_0}\,dx' \tag{28}$$

and

$$\tau_n=\left[\frac{\alpha}{2\omega_0}\right]\int_c^d\frac{dx'}{\sqrt{(n+\frac{1}{2})-V(x')/\hbar\omega_0}} \ . \tag{29}$$

Here, η_n is the phase accumulated from traversing the classically allowed region between the barrier and the continuum; τ_n is the respective classical transit time across the same region.

Similarly, the wave vector k may be expanded about ω, yielding

$$k=k_n+\gamma_n[\omega-(n+\tfrac{1}{2})\omega_0] \ , \tag{30}$$

where

$$k_n=\alpha\left[n+\frac{1}{2}+\frac{\phi}{\hbar\omega_0}\right]^{1/2} \tag{31}$$

and

$$\gamma_n=\frac{\alpha^2}{2\omega_0 k_n} \ . \tag{32}$$

By extending the limits of integration in Eq. (24) to infinity and making use of these results, the integral can easily be evaluated by the method of residues. Retaining only the term representing a wave traveling to the right, and removing the slowly varying term $k^{-1/2}$ from the integral, the final expression for the propagator is

$$G(x',x;t)=\left[\frac{\alpha}{4\pi}\right]^{-1/2}\sum_{n=0}^{N}\left[n+\frac{1}{2}+\frac{\phi}{\hbar\omega_0}\right]^{-1/4}\theta_n^{-1}\psi_n^{\mathrm{LHO}}(x')e^{i[k_n(x-d)+\eta_n]}$$
$$\times e^{-i(n+\frac{1}{2})\omega_0 t}e^{-(\Gamma_n/2)[t-\tau_n-\gamma_n(x-d)]}\Theta[t-\tau_n-\gamma_n(x-d)] \ . \tag{33}$$

Here, $\Theta(x)$ is the Heaviside step function. The arbitrary exponential phase factor $\pi/4$ in Eq. (24) has been ignored.

The propagator in Eq. (33) consists of a superposition of exponentially decaying traveling waves which are delayed by corresponding classical transit times from the edge of the barrier to the continuum region. Each of the quasibound states decays with the usual WKB decay rate given by Eq. (26). The sharp turn-on of each quasibound state is related to the simple pole approximation used to evaluate the propagator. We point out that these results are also valid when the continuum lies above the bottom of the well ($\phi<0$) if the lower limit in the summation in Eq. (33) is replaced by the lowest LHO level which lies above the continuum energy. True LHO bound states in the well which lie below the continuum decay exponentially in the region $x>b$ in Fig. 1 and make negligible contributions to the probability beyond the barrier.

C. Tunneling probability

Application of Eqs. (3) and (33) to an arbitrary wave packet composed of LHO eigenstates with probability amplitudes c_n reveals that, beyond the barrier, $\Psi(x,t)$ in Eq. (33) is simply a superposition of tunneling components weighted by their appropriate c_n. The probability of escape for a wave packet initially localized in the well is defined to be

$$P(t)=\int_d^L|\Psi(x',t)|^2dx' \ . \tag{34}$$

Ignoring the rapid interference modulations between different quasibound states, this gives a tunneling probability of

$$P(t)=\frac{\sum_{n=0}^{N}|c_n|^2[1-e^{-\Gamma_n(t-\tau_n)}]\Theta(t-\tau_n)}{\sum_{n=0}^{N}|c_n|^2} \ , \tag{35}$$

when normalized to the probability of the initial wave packet lying below the barrier. This result is easily interpreted. The tunneling probability is simply the sum of the individual probabilities for each of the exponentially decaying quasibound states to tunnel through the barrier, weighted by the probability of the wave packet to be in that particular quasibound state. As $t\to\infty$, the probability in Eq. (35) approaches unity.

III. TUNNELING OF SQUEEZED STATES

A. Tunneling times

To investigate the significance of squeezing on tunneling times, we calculate the tunneling probability in Eq. (35) for the case in which the initial state $\Psi(x,0)$ is a squeezed state. To do this, we evaluate θ and η for the specific case of a cubic barrier coupled to a flat continu-

um (Fig. 1). The barrier is assumed to have a height $V_0 = 10\hbar\omega_0$, and we take the number of corresponding quasibound states to be $N = 10$. Details of the evaluation of barrier quantities are presented in Appendix B.

We consider only pure amplitude and phase-squeezed states. The initial squeezed wave packet can be represented as [11]

$$\Psi(x,0) = (2\pi)^{-1/4}(\alpha S)^{1/2} e^{-(\alpha S x/2 - \beta)^2} . \quad (36)$$

The standard deviation Δx of wave-packet position within the parabolic well is $(\alpha S)^{-1}$, where S is related to a squeezing parameter R which is a linear measure of squeezing and defined by the relation $S = e^R$ [11]. If $S < 1$, the wave packet is phase squeezed and characterized by a Δx greater than the ground-state standard deviation. If $S > 1$, amplitude squeezing applies, and Δx is smaller than the ground-state standard deviation. The initial mean displacement in $2\beta(\alpha S)^{-1}$.

The initial squeezed state may easily be represented in terms of LHO states with probability amplitudes which can be calculated by various methods [11,12]. Tunneling escape times τ_t, arbitrarily defined by the condition

$$P(\tau_t) = 1 - e^{-1} , \quad (37)$$

may then be calculated by direct application of Eq. (35). This definition of escape time permits direct comparison with the purely exponential decay of LHO eigenstates. The tunneling escape times for various degrees of squeezing versus average energy are plotted in Fig. 2, together with tunneling times for eigenstates of the parabolic well. Figure 3 reveals that the tunneling times for squeezed states reach a minimum at $S \approx 1.5$ for an average energy $E = 4.5\hbar\omega_0$. Interestingly, this does not correspond to the case of a pure coherent state ($S = 1.0$). Instead, it corresponds closely to the value of S at which energy fluctuations reach a minimum, as indicated in Fig. 4 and discussed below.

To understand first how squeezing affects the energy distribution, we consider the relationship between squeezing and the energy variance $\langle (\Delta E)^2 \rangle$. This is given by

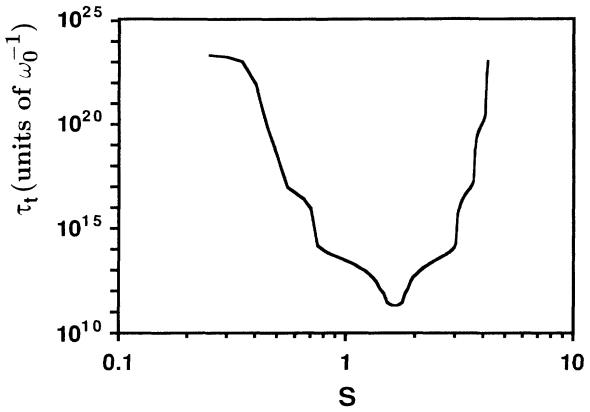

FIG. 3. Example of tunneling escape times versus squeezing parameter for an arbitrary fixed energy $E = 4.5\hbar\omega_0$.

the expression [12]

$$\langle (\Delta E)^2 \rangle = \tfrac{1}{8}(\hbar\omega_0)^2[(8\beta^2+1)S^{-4} + S^4 - 2] . \quad (38)$$

The energy of a squeezed state is given by a similar expression,

$$\langle E \rangle = \tfrac{1}{4}\hbar\omega_0[(4\beta^2+1)S^{-2} + S^2] . \quad (39)$$

The average energy in Eq. (39) depends both on the initial mean displacement of the squeezed state $2\beta(\alpha S)^{-1}$ as well as the position and momentum uncertainties, Δx and Δp. These in turn are proportional to S^{-1} and S, respectively. These uncertainties contribute additional kinetic and potential energy to the wave packet, increasing its energy above that of a pure coherent state with displacement β.

From Eq. (39), we see that for small displacements β the energy is dominated by uncertainties in position and momentum. For small energies ($2\beta S^{-1} \approx 0$), these uncertainties contribute equally to potential energy $(\Delta x)^2$ and kinetic energy $(\Delta p)^2$. Thus, for small energies, the total fluctuation in energy is minimized when potential and kinetic energy fluctuations are simultaneously minimized,

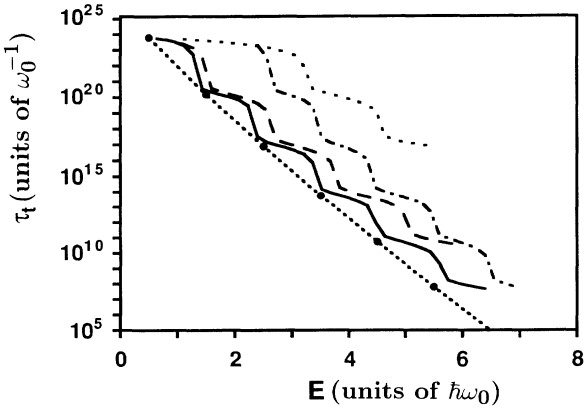

FIG. 2. Tunneling escape times versus energy for cubic barrier, plotted for various values of squeezing: $S = 0.5$ (solid), 1.0 (dashed), 1.5 (dotted), and 3.0 (chain). Barrier and continuum parameters are $V_0 = 10\hbar\omega_0$, $N = 10$, and $\phi = 2\hbar\omega_0$.

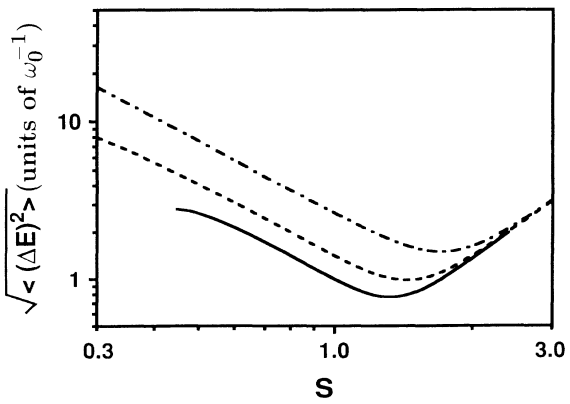

FIG. 4. Energy fluctuations of a squeezed state versus squeezing parameter S. The three curves correspond to different particle energies: $E = 2.0$ (solid), 5.0 (dashed), and 50 (dotted).

or S is close to one. On the other hand, for larger initial displacements ($2\beta S^{-1}>0$), the potential energy acquires contributions not only from position and momentum uncertainties, but from the mean displacement itself. Furthermore, large wave-packet displacements increase the *slope* of the potential energy curve, amplifying the contributions of positional fluctuations Δx. Thus, at large average energies ($2\eta S^{-1}\gg 0$), fluctuations of potential energy are weighted more heavily than fluctuations of kinetic energy. In this way, energy fluctuations can be expected to minimize for a value of S greater than one, in agreement with an algebraic minimization of Eq. (38) with respect to S which furnishes the result $S_{\min}=(1+8\beta^2)^{1/8}$.

The corresponding minimization of tunneling times occurs as a result of the LHO occupation probability distributions narrowing to a small number of LHO quasibound states as S approaches $S_{\min}$ (Fig. 5). Quasibound-state tunneling probabilities for neighboring levels vary by several orders of magnitude, so a wave packet composed of a wide distribution of LHO states requires many very long-lived quasibound states to decay before the tunneling probability becomes appreciable. However, for squeezed wave packets with $S\approx S_{\min}$, only a few short-lived, quasibound states need to decay before the wave packet has tunneled significantly. This also explains why LHO eigenstates have the shortest tunneling escape times for a given energy, as seen in Fig. 2.

In addition to the sensitivity of wave-packet escape times on squeezing, the tunneling escape times plotted in Fig. 2 also exhibit interesting steplike features near quasi-bound-state energies. These steps are related to the decomposition of the initial squeezed state into a superposition of discrete quasibound states. A squeezed state dominated by a single quasibound state exhibits tunneling behavior dominated by that level. If the average energy is increased by some fraction of $\hbar\omega_0$, then additional levels must be occupied significantly to account for this additional energy. Because of the very large differences in tunneling rates between neighboring LHO levels, significant changes in tunneling rates are to be expected as higher LHO levels become significantly occupied.

For large amounts of phase squeezing ($S=0.5$, Fig. 2) the steps in tunneling time become less prominent and do not occur at every LHO eigenenergy. Under these conditions, the broad energy distributions of phase-squeezed states cover more than one LHO level spacing so that the correspondence between particular quasibound states and individual steps is lost. The tunneling time also exhibits steplike features as a function of squeezing for fixed energies, as depicted in Fig. 3. These features similarly arise from changes in occupation of LHO discrete levels as the amount of squeezing is varied.

B. Coherences

Coherent effects become evident when the properties of the tunneled wave function can be resolved on time scales on the order of ω_0^{-1} and length scales on the order of α^{-1}. For example, the probability $|\psi(x,t)|^2$ for a pure coherent state develops deep modulations at the wave-packet oscillation frequency ω_0 as shown in Fig. 6. These modulations arise from interferences between adjacent quasibound states.

Wave-packet squeezing can emphasize higher harmonics of ω_0 and alter the shape of tunneling modulations. These effects are apparent in Figs. 7(a)–7(d), where $|\psi(x,t)|^2$ is plotted for $x=d$ with various degrees of squeezing at a fixed energy close to the LHO ground-state energy. Figure 7(a) depicts a pure coherent state with modulations at ω_0, consistent with the purely oscillatory motion of the wave-packet mean $\langle x(t)\rangle$ in the well. As the wave packet becomes amplitude squeezed, the wave-packet variance $\langle[\Delta x(t)]^2\rangle$ begins to oscillate at $2\omega_0$, so that second harmonic modulations begin to appear in the tunneling probability beyond the barrier [Fig. 7(b)]. Similarly, phase squeezing introduces second harmonics, but with the phase reversal evident in Fig. 7(c).

With maximum squeezing ($\beta=0$), wave packets localized in the well consist of superpositions of even harmonics only, with the result that breathing-type oscillations in $\langle[\Delta x(t)]^2\rangle$ occur purely at $2\omega_0$ as shown in Fig. 7(d). At higher energies, these coherent effects become less pro-

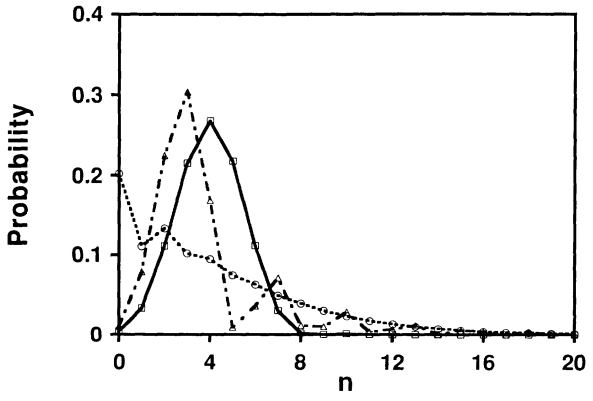

FIG. 5. Probability distribution $|c_n|^2$ for squeezed states versus occupation number n, plotted for various values of squeezing: $S=0.5$ (circles), 1.5 (squares), and 3.0 (triangles) with arbitrary fixed energy $E=4.5\hbar\omega_0$. The curves are to guide the eye.

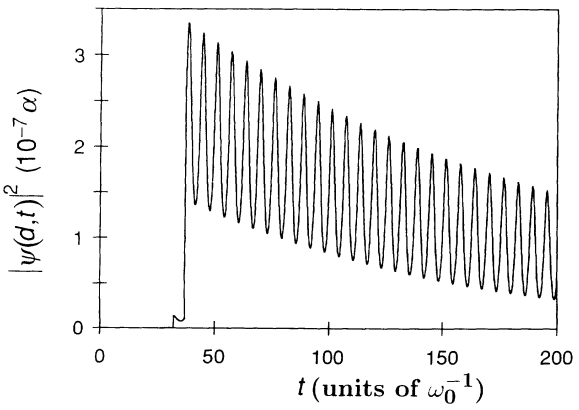

FIG. 6. Probability $|\psi(d,t)|^2$ of particle detection at point d beyond the barrier as a function of time for a coherent state with $S=1.0$ and energy $E=0.6\hbar\omega_0$. Barrier and continuum parameters are $V_0=4\hbar\omega_0$, $N=4$, and $\phi=2\hbar\omega_0$.

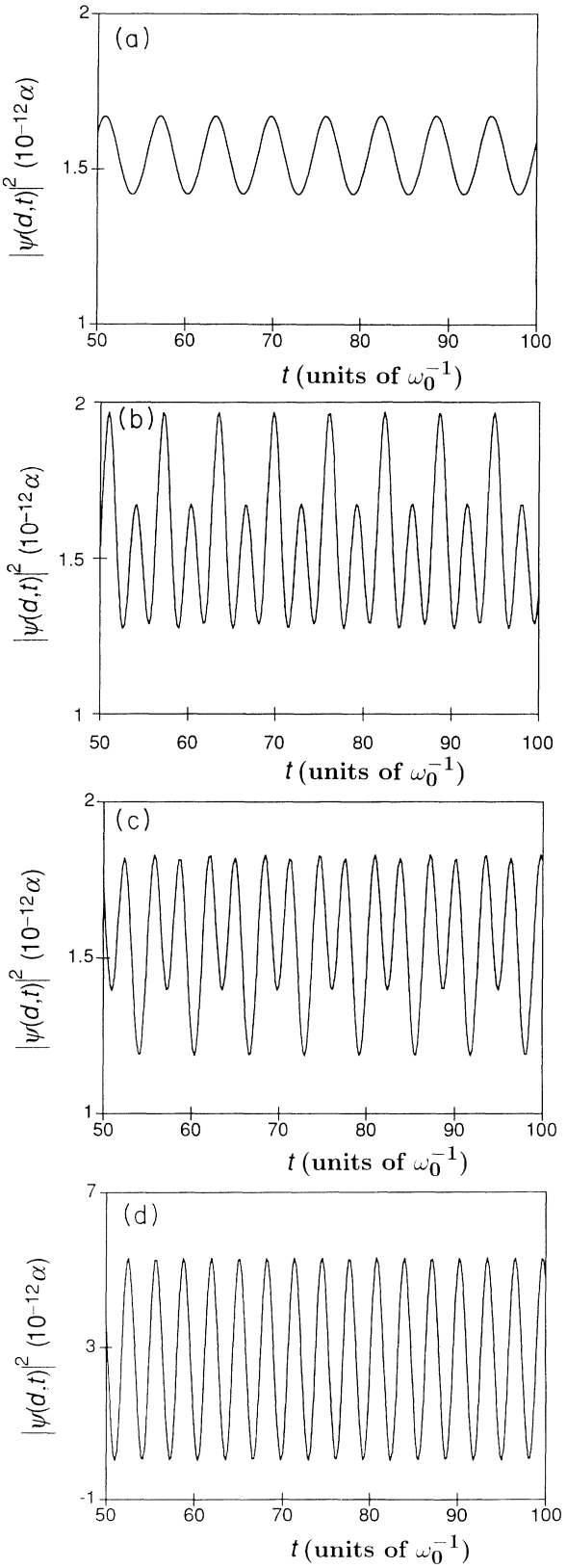

FIG. 7. Probability $|\psi(d,t)|^2$ for various degrees of squeezing and initial displacements β for particle energies exceeding the ground-state energy $E_g = 0.5\hbar\omega_0$ by only $\Delta E = 10^{-6}\hbar\omega_0$: (a) $S = 1.0000$, $\beta = 10^{-3}$; (b) $S = 1.0001$, $\beta = 9.95 \times 10^{-4}$; (c) $S = 0.9999$, $\beta = 9.95 \times 10^{-4}$; and (d) $S = 1.0010$, $\beta = 0$. Barrier and continuum parameters are $V_0 = 4\hbar\omega_0$, $N = 4$, and $\phi = 2\hbar\omega_0$.

nounced as excited quasibound states become progressively more populated. This occurs because θ_n^{-2} increases exponentially with energy level n and dominates the behavior of the tunneling probability contributions $\theta_n^{-2}|c_n|^2$ at higher energies, reducing modulation contrast. Modulations become large only when the probabilities $|c_n|^2$ decrease rapidly enough to counterbalance the θ_n^{-2} term in $\theta_n^{-2}|c_n|^2$. For squeezed states tunneling through a cubic barrier, this occurs at average particle energies approaching that of the ground state.

IV. DISCUSSION AND CONCLUSIONS

The results obtained in this paper have interesting implications for quantum control [13] of chemical systems with effective potentials of the general form shown in Fig. 1, where an energy barrier separates the initial from the final state. For example, simple molecules such as diatomic alkali metals occasionally have excited-state potentials with centrifugal barriers separating shallow quasibound regions from dissociative continua. The $^1\Pi_u$ state of Cs_2 accessed at 766.7 nm, for example, has a potential of this type [14]. In principle, for excited-state potential wells deep enough to contain several vibrational states, dissociative dynamics would then depend on the detailed nature of the initial wave packet.

Our results are most relevant, however, to cases of very deep potential wells with part or all of the well located above the dissociative asymptote. This situation is more typical of predissociative states of simple molecules like IBr (electronic predissociation [15]) and HgH (vibrational dissociation [16]). Examples among the diatomic alkali metals include the $C\ ^1\Pi_u$ state of Cs_2 [17] and the $6\ ^1\Sigma_g^+$ state of Na_2 [18] which form adiabats through avoided crossings with repulsive states similar to the model considered here. The influence of tunneling was specifically considered as early as the work of Farkas and Levy [19] on AlH. In such systems, our calculations indicate that initial-state preparation strongly affects the evolution of excited-state reactions. Both the amplitude and phase of individual quasibound states encompassed in the initial superposition state affect the rate of tunneling through the barrier. Reaction time scale and yield should therefore be amenable to manipulation using incident light pulses of durations less than a vibrational period with tailored amplitude, bandwidth, central frequency, and chirp to slow down or speed up chemical dynamics. In optically initiated unimolecular reactions, ultrafast dissipation of excitation to intramolecular vibrational reservoirs should be impeded by appropriate phase and chirp manipulation of incident pulses. This suggests useful extensions of the experimental techniques developed recently [20] for molecular wave-packet preparation, to exploit optical phasing in the creation of squeezed matter states analogous to squeezed states of the radiation field [11] with correspondingly modified, nonclassical dynamics.

The modification of tunneling dynamics by squeezing also has interesting consequences for dc-biased Josephson junctions and Josephson interferometers and is particularly germane to precision measurements of magnetic flux or voltage close to the shot-noise limit with these struc-

tures [21]. Here, the relevant variable is the Cooper pair center-of-mass phase difference δ in the BCS ground-state wave functions on either side of the Josephson barrier [22]. The dynamics of the phase difference δ arise from a quantum-mechanical "binding energy" $V(\delta)$ due to coupling of Cooper pairs on either side of the barrier by the tunneling interaction [23]. These dynamics have been studied extensively in both the classical regime [24] and more recently in the quantum regime at low temperatures where quantized energy levels observed in interactions with microwave radiation [25] and tunneling of the phase difference δ from potential minima in $V(\delta)$ have been observed [26].

The tunneling dynamics of the phase difference δ and corresponding junction voltage $V=(\hbar/2e)\dot{\delta}$ across a Josephson junction with capacitance C can be described by an effective quantum-mechanical Hamiltonian consisting of a potential energy

$$V(\delta)=-E_J(\cos\delta+\delta I/I_J) \tag{40}$$

and a kinetic charging energy $(2en)^2/2C$, where $2en$ is the amount of charge transferred across the junction, $I_J=2eE_J/\hbar$, and E_J is a constant related to the tunneling interaction matrix elements and density of states [23,27,28]. When the applied current I is less than I_J in Eq. (40), the potential $V(\delta)$ is locally well approximated by a cubic potential of the form shown in Fig. 1 with $\phi \gg \hbar\omega_0$. The preparation of squeezed states $\psi(\delta)$ should then be feasible by application of a constant bias current and a microwave current at $2\omega_0$ to modulate the resonant frequency of the "quantum well" [25] $\omega_0=(2\sqrt{2}eI_JC/\hbar)^{1/2}(1-I/I_J)^{1/4}$ together with seed currents at ω_0 to provide additional control of mean wave-packet displacement and phasing. This is closely analogous to optical [5] and microwave squeezing [29] by parametric interactions.

The results of this work indicate that large amounts of phase squeezing ($S \gg 1$) would strongly inhibit tunneling decay in a potential of the form given in Eq. (40), and permit improved ultralow-noise measurements of weak signals at low temperatures by squeezed states whose noise properties are well known to be highly affected by loss [30]. Furthermore, we expect these results to be important in fundamental dynamics of coupled junctions where wave-packet localization can be expected to enhance or inhibit tunneling in a fashion reminiscent of numerical simulations of forced double potential wells [31].

Optical crystals, formed by trapping laser-cooled atoms in periodic optical potential wells, constitute another system in which squeezing of atomic states could significantly affect tunneling. In this case, tunneling occurs as nonclassical motion of escaping atoms or those moving between minima of the optical field configuration. Recent results have demonstrated quantized motion of atoms trapped within optical potential wells, indicated by the presence of vibrational sidebands in resonance fluorescence spectra or in stimulated Raman spectra [32]. Just as for quasibound states of molecules, the induced vibrational manifolds of such atoms should be amenable to preparation of squeezed vibrational states [7]. The results of the present work indicate that squeezing of trapped atoms could strongly influence their tunneling rates into neighboring wells as well as their escape from the trap.

In summary, we have calculated tunneling times for squeezing states initially confined to a harmonic potential well coupled to a continuum. The fastest tunneling rates are observed for wave packets prepared with small amounts of amplitude squeezing, but their rates never exceed those of pure LHO eigenstates. On the other hand, tunneling is inhibited by large squeezing. We have also elucidated the relationship between the energy dispersion of wave packets and tunneling rates, as well as more subtle steplike behavior arising from the discrete nature of quasibound states in the well. Oscillatory behavior of the wave packet can give rise to modulations in the tunneling wave-function probability which are most visible when relative contributions to excited-state populations decrease exponentially with increasing vibrational quantum number. Finally, applications of squeezed matter wave packets have been identified for control of excited-state chemical reactions by appropriately tailored ultrafast light pulses, modification of macroscopic tunneling dynamics in Josephson junctions, and inhibition of tunneling of trapped atoms in optical crystals.

ACKNOWLEDGMENTS

The authors gratefully acknowledge E. Ben Jacob for suggesting this problem and for many helpful discussions. We would also like to thank K. T. Hecht for helpful conversations. Partial support of this research was provided by the Air Force Office of Scientific Research (H. Schlossberg).

APPENDIX A

The question of normalization of wave functions may be handled by first matching the WKB solutions $U_{k_n}(x)$ to the normalized LHO eigenstates in the semiclassical limit. By explicit integration, the WKB solution in Eq. (8) for a parabolic well yields

$$U_{k_n}^{\mathrm{II}}(z)=(2\alpha)^{1/2}\left[4\left[n+\frac{1}{2}\right]-z^2\right]^{-1/4} \times\cos\left[\frac{\pi}{4}-\frac{\pi}{2}\left[n+\frac{1}{2}\right]+\vartheta\right], \tag{A1}$$

where $z=\alpha x$. The phase ϑ is given by

$$\vartheta=-\frac{z}{4}\left[4\left[n+\frac{1}{2}\right]-z^2\right] + \left[n+\frac{1}{2}\right]\sin^{-1}\left[\frac{z}{2(n+\frac{1}{2})}\right]. \tag{A2}$$

In the limit of large quantum numbers, this result matches the asymptotic expansion for the parabolic cylinder functions $D_n(-z)$ to within a constant of pro-

portionality [33]. For integer values of n, the parabolic cylinder functions reduce to Hermite-Gaussian LHO solutions. Comparing the WKB solution in Eqs. (A1) and (A2) to the normalized asymptotic LHO solutions for integer n reveals

$$U_n(x)=2(-1)^n\pi^{1/2}\alpha^{-1}\psi_n^{\mathrm{LHO}}(x), \quad x<c \tag{A3}$$

where

$$\psi_n^{\mathrm{LHO}}(x)=2^{-n/2}(2\pi)^{-1/4}\alpha^{1/2}e^{-\alpha^2x^2/4}\mathrm{H}_n(\alpha x/\sqrt{2}) . \tag{A4}$$

Here, $\mathrm{H}_n(x)$ are Hermite polynomials of order n.

We can now calculate the normalization constant A_0 for the on-resonance and off-resonance cases by integrating $|\psi(x)|^2$ in Eq. (6) over all space. When the resonance condition $\xi=\pi(n+\frac{1}{2})$ is not met, only the wave-function amplitude in continuum region contributes significantly to the total wave-function probability. Integrating $|U_k^{\mathrm{V}}(x)|^2$ over the continuum region gives the off-resonant result in Eq. (20). However, close to quasi-bound-state resonances, the wave-function amplitude in the well region becomes appreciable. Replacing the WKB wave functions in the well region [Eqs. (7)–(9)] with the LHO wave functions normalized to the WKB solutions in Eq. (A3), we find A_0 is approximately

$$A_0=\left[4\pi\alpha^{-1}\int_{-\infty}^{d}|\psi_n^{\mathrm{LHO}}(x')|^2dx' + \int_d^L|U_{k_n}^{\mathrm{V}}(x')|^2dx'\right]^{-1/2}, \quad \xi\approx\pi(n+\tfrac{1}{2}) . \tag{A5}$$

The small contributions just beyond the barrier (region IV) have been neglected. Evaluating Eq. (A5) explicitly yields the result for the on-resonant case in Eq. (20).

APPENDIX B

In this appendix, we compute the barrier parameters for the specific case of a cubic potential. The cubic potential in Fig. 1 has the general form

$$V(x)=(27V_0/4)x^2(w-x)/w^2 . \tag{B1}$$

At the LHO eigenenergies $E=\hbar\omega_0(n+\frac{1}{2})$, the tunneling parameter [Eq. (15)] is

$$\theta_n=\exp\left[\alpha\int_b^c\sqrt{V(x)/\hbar\omega_0-(n+\tfrac{1}{2})}dx'\right] , \tag{B2}$$

where b and c are the barrier turning points. To obtain accurate results for intermediate energies, the integral in (B2) is evaluated exactly. This can be performed by factoring the cubic polynomial in the radical of the integrand in Eq. (B2). The zeros of the polynomial are simply the three turning points a, b, and c. The integral can be expressed in terms of the Gauss-hypergeometric function [34]. The resulting tunneling parameter becomes

$$\theta_n=\exp(I_n) , \tag{B3}$$

where I_n is

$$I_n=\left[\frac{\pi}{4}\right]B^2(y_2-y_1)^{1/2}(y_3-y_2)^2 \times{}_2F_1\left[-\frac{1}{2},\frac{3}{2};3;-\frac{y_3-y_2}{y_2-y_1}\right] . \tag{B4}$$

The parameters $y_3>y_2>y_1$ are the turning points in units of w and are roots of the cubic equation

$$B^2y^2(y-1)+(n+\tfrac{1}{2})=0 . \tag{B5}$$

The constant B is given by

$$B=\sqrt{27V_0/4\hbar\omega_0} . \tag{B6}$$

The phase parameter η_n and the classical delay time τ_n, given by Eqs. (28) and (29), are most easily evaluated by assuming the potential in region IV of Fig. 1 is linear. We simply state the results:

$$\eta_n=\left[\frac{4}{3B}\right]\left[\eta+\frac{1}{2}+\frac{\phi}{\hbar\omega_0}\right]^{3/2} \tag{B7}$$

and

$$\tau_n=2B\omega_0\left[n+\frac{1}{2}+\frac{\phi}{\hbar\omega_0}\right]^{3/4} . \tag{B8}$$

[1] E. H. Kennard, Z. Phys. **44**, 326 (1927).
[2] E. Takahashi, in *Advances in Communications Systems*, edited by V. Balakrishnan (Academic, New York, 1965), p. 227.
[3] R. E. Slusher, L. W. Hollberg, B. Yurke, J. C. Mertz, and J. F. Valley, Phys. Rev. Lett. **55**, 2409 (1985).
[4] R. M. Shelby, M. D. Levenson, S. H. Perlmutter, R. G. Devoe, and D. F. Walls, Phys. Rev. Lett. **57**, 691 (1986).
[5] L. A. Wu, H. J. Kimble, J. L. Hall, and H. Wu, Phys. Rev. Lett. **57**, 2520 (1986).
[6] Y. Yamamoto, S. Machida, and O. Nilsson, Phys. Rev. A **34**, 4025 (1986).
[7] J. I. Cirac, A. S. Parkins, R. Blatt, and P. Zoller, Phys. Rev. Lett. **70**, 556 (1993).
[8] H. Dekker, Phys. Lett. A **119**, 10 (1986).
[9] D. Mugnai, A. Ranfagni, M. Montagna, O. Pilla, and G. Viliani, Phys. Rev. A **40**, 3397 (1989).
[10] E. Merzbacher, *Quantum Mechanics* (Wiley, New York, 1970), p. 121.
[11] H. P. Yuen, Phys. Rev. A **13**, 2226 (1976).
[12] R. W. Henry and S. C. Glotzer, Am. J. Phys. **56**, 318 (1988).
[13] W. S. Warren, H. Rabitz, and M. Dahleh, Science **259**, 1581 (1993).
[14] P. Kusch and M. Hessel, J. Mol. Spectrosc. **32**, 181 (1969).
[15] M. B. Faist and R. B. Bernstein, J. Chem. Phys. **64**, 2971 (1976).
[16] G. Herzberg, *Spectra of Diatomic Molecules* (Van Nostrand Reinhold, Toronto, 1950), p. 427.
[17] G. Rodriguez and J. G. Eden, Chem. Phys. Lett. **205**, 371 (1993).
[18] C.-C. Tsai, J. T. Bahns, and W. C. Stwalley, J. Chem.

Phys. (to be published); C.-C. Tsai, J. T. Bahns, T.-J. Whang, H. Wang, and W. C. Stwalley, Phys. Rev. Lett. (to be published).

[19] L. Farkas and S. Levy, Z. Phys. **84**, 195 (1933).

[20] T. J. Dunn, J. N. Sweester, I. A. Walmsley, and C. Radzewicz, Phys. Rev. Lett. **70**, 3388 (1993); M. Dantus, M. J. Rosker, and A. H. Zewall, J. Chem. Phys. **87**, 2395 (1987).

[21] S. T. Pavlov and A. V. Prokhorov, Fiz. Tverd. Tela (Leningrad) **33**, 2460 (1991) [Sov. Phys. Solid State **33**, 1384 (1991)]; **34**, 97 (1992) [**34**, 50 (1992)].

[22] R. P. Feynman, *Statistical Mechanics* (Benjamin, Reading, MA, 1972).

[23] D. J. Scalapino, in *Tunneling Phenomena in Solids,* edited by E. Burnstein and S. Lundqvist (Plenum, New York, 1969), Chap. 32.

[24] D. N. Langenberg, in *Tunneling Phenomena in Solids,* edited by E. Burnstein and S. Lundqvist (Plenum, New York, 1969), Chap. 33.

[25] M. H. Devoret, J. M. Martinis, D. Esteve, and J. Clarke, Helv. Phys. Acta **61**, 622 (1988).

[26] R. F. Voss and R. A. Webb, Phys. Rev. Lett. **47**, 265 (1981); D. Esteve, J. M. Martinis, C. Urbina, E. Turlot, M. Devoret, H. Grabert, and S. Linkwitz, Phys. Scr. **129**, 121 (1989).

[27] A. O. Caldeira and A. J. Leggett, Ann. Phys. (N.Y.) **149**, 374 (1983).

[28] E. Shimshoni and E. Ben-Jacob, Phys. Rev. B **43**, 2705 (1991).

[29] R. Movshovich, B. Yurke, P. G. Kaminsky, A. D. Smith, A. H. Silver, R. W. Simon, and M. V. Schneider, Phys. Rev. Lett. **17**, 1419 (1990).

[30] L. Wu, M. Xiao, and H. J. Kimble, J. Opt. Soc. Am. B **4**, 1465 (1987).

[31] W. A. Lin and L. E. Ballentine, Phys. Rev. Lett. **65**, 2927 (1990).

[32] P. S. Jessen, C. Gerz, P. D. Lett, W. D. Phillips, S. L. Rolston, R. J. C. Spreeuw, and C. I. Westbrook, Phys. Rev. Lett. **69**, 49 (1992); P. Verkerk, B. Lounis, C. Salomon, C. Cohen-Tannoudji, J. Courtois, and G. Grynberg, *ibid.* **68**, 3861 (1992); G. Grynberg, B. Lounis, P. Verkerk, J.-Y. Courtois, and C. Salomon, *ibid.* **70**, 2249 (1993).

[33] *Handbook of Mathematical Functions,* edited by M. Abramowitz and I. A. Stegun (Dover, New York, 1970), p. 690.

[34] I. S. Gradshteyn and I. M. Ryzhik, *Tables of Integrals, Series, and Products* (Academic, Orlando, 1980).